Characterizing the dynamic behavior and performance of a scaled prototype point absorber wave energy converter in a large wave flume

Giorgio Bacelli, Max Ginsburg, Alex Haegmueller, and Budi Gunawan

Abstract—A scaled point absorber wave energy converter with advanced control system was tested at a large wave flume for obtaining datasets that will be used for designing the WEC power take-off (PTO). To help achieve the testing goal, an analytical model to describe the input and output behavior of the WEC system was developed. The analytical model consists of two parts: a hydro-mechanical part that describes the wave-body interaction of the WEC, and an electromechanical part that describes the WEC PTO dynamics. System identification analyses were used in conjunction with experimental datasets to derive model parameters. A set of regular and irregular wave cases were designed and selected for developing multiple power generation performance curves for three different tuning variables: spring stiffness, PTO damping and spring pretension force. The analyses of the performance curves for selecting optimal performance and cost balance are described in details.

Keywords—WEC control; close looped; wave testing; power take-off; wave energy

I. Introduction

DESIGNING a wave energy converter (WEC) often involves characterizing the dynamic behavior and performance of a scaled prototype of the WEC in order to de-risk a development project. This paper presents a scaled prototype testing of a second generation point-absorber WEC, designed by AquaHarmonics, Inc., at the Oregon State University's large wave flume. The second generation AquaHarmonics WEC has a similar working mechanism as to the first generation AquaHarmonics WEC that was awarded the first prize during the Wave Energy Prize competition [1], but with improved hardware and protocols. The main objectives of the tests are to verify the performance of the AquaHarmonics' scaled wave energy converter with control system enabled (in closed loop operations), and to gather datasets that will be used for designing the WEC

Power Take Off (PTO) at a larger scale, suitable for open water testing.

II. Device Description

AquaHarmonics' wave energy device (the "device") is a point absorber comprised of a 120 degree symmetrical cone shape for the bottom and top portion of the hull with a cylinder shaped section connecting the top and bottom portions of the hull (Fig. 1). The power take-off (PTO) is comprised of a large diameter, narrow width sheave fixed to a shaft and supported by bearings in a sealed compartment which is integrated into the lower portion of the hull (Fig. 2). The main PTO mooring line is connected at one termination to a buoyant connection assembly at the end of the mooring chain, enters the device through an opening at the bottom center of the hull and then passes through a roller fairlead assembly mounted at the base of the sealed PTO compartment. It then wraps around the PTO sheave up to four times, and finally terminates at a connection point inside the PTO sheave.

The opposite ends of the PTO shaft are directly coupled to two direct drive, multi-stage, axial flux outer stator permanent magnet generators which have been in development for use in the wind power industry as a next generation solution to the standard generator/gearbox arrangement currently used. The ability to eliminate the gearbox at this scale of power leads to an increase in overall system reliability and simplicity, as well as capital cost reduction. Mounted directly to the PTO shaft is a return spring that provides the minimum necessary return force and stored energy to reel in the main PTO line. This increases device efficiency over utilizing only the device PTO generators for return the device, as well as making zero velocity point detection easier and simpler for the control system.

The device is free-floating in 6 degrees of freedom (DOF) and generates power in the heave DOF, with some power generated in the surge & sway components of the device

motion for 3 DOF power production. The device is designed to produce power only on the up-swell of the wave by generating high tensile forces in the main PTO mooring line between the device and the embedded anchor plate, which rotates the PTO sheave in its bearings and produces high torque, low RPM power at the directly driven generators, as well as storing energy in the return spring system. On the down-swell of the wave the device operates in a PTO "motoring" condition by a combination of releasing energy stored in the return spring system and powering the generators in the opposite direction to return the device to its home position at the bottom of the wave by reeling in the main PTO mooring line. The power production cycle is then restarted. The amount of electric return force is modified depending on the wave period and amplitude.

The power leads of the generators are connected to a solid state control system. The control system consists of a microcomputer running proprietary code that switches the generators between power generation and motoring /winching modes/braking by monitoring motor current, velocity, and motion of the device itself through an inertial measurement unit (IMU). The control system also conditions the power prior to being sent to shore or to a floating power processor via the shore power cord that is run along one of the non-primary wave propagation catenary mooring lines.

The device is designed to have enough of the main PTO mooring line in storage on the PTO sheave such that it will never encounter an end-stop event in the range of waves within the scope of the Wave Energy Prize, and beyond. The device as shown at full scale has a total usable stroke of 43 meters. The function of the device in normal operation also compensates for tidal and current changes. For the 1/20th scale model, total stroke of the PTO will be 1.15m.

Mounted directly to the PTO shaft is a return spring that provides the minimum necessary return force and stored energy to reel in the main PTO line. This increases device efficiency over utilizing only the device PTO generators for return the device, as well as making zero velocity point detection easier and simpler for the control system.
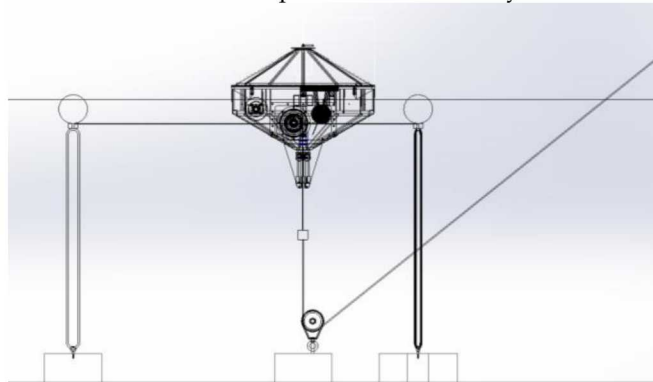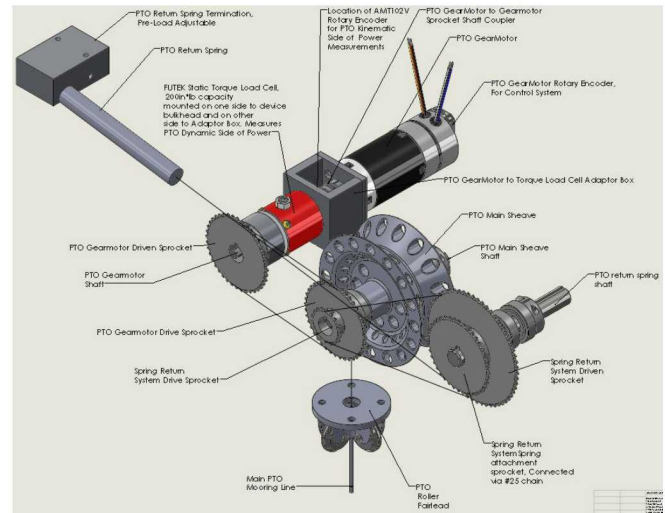

Fig. 2. PTO layout and description.

III. TESTING SETUP AND METHOD

The testing was conducted in the Large Wave Flume at Oregon State University's (OSU) O.H. Hinsdale Wave Research Laboratory (HWRL) in Corvallis, Oregon. The flume is 104 m long, 3.7 m wide, and has a maximum depth of 4.6 m (Fig. 3). The flume's wave maker is a hydraulically actuated piston type wavemaker, capable of making regular, irregular, Tsunami, and user defined waves in the range of periods from 0.8 to 12 seconds. The wavemaker is capable of making a 1.7 m wave in a maximum water depth of 2.7 m. It has a carriage for personnel access to instrumentation as well as an overhead gantry crane.

With respect to the tank test in the Large Wave Flume, the reference frame of the device is illustrated in figure 4. The device operational origin is located at the device center of gravity, based on the static water line of the device with only the mechanical PTO spring preload set. The +X axis is aligned with the flume, away from the wave maker, and the positive y-axis is perpendicular to the flume wall as shown in Fig. 4. Waves propagating parallel with the x-axis (toward the beach) are defined as having a mean wave direction of zero degrees. This convention defines the wave direction as the direction the waves are traveling toward.

Fig. 3. The Large Wave Flume at Oregon State University's Hinsdale laboratory.

Fig. 1. A schematic side view of AquaHarmonics device showing the main PTO line and catenary mooring lines.
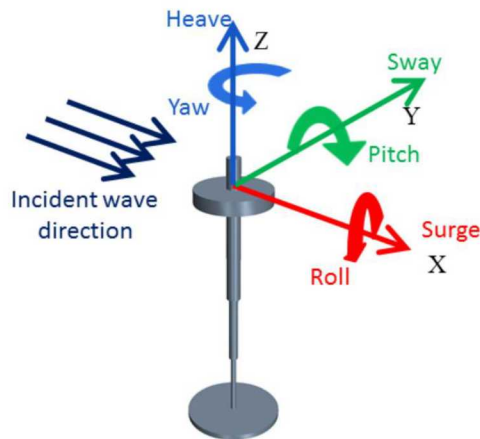
Fig. 4. Device reference frame used for testing at the Large Wave Flume [2].

The verification of the closed loop performance of the WEC was evaluated qualitative and quantitatively. The qualitative evaluation was conducted by observing the device behavior during testing, i.e. the device operated correctly as expected/prescribed, without unexpected vibrations of the PTO (instability) and without excessively large oscillations in modes other than heave.

In order to quantitatively evaluate the closed loop performance of the WEC the control system has been implemented as a feedback system consisting of a Proportional Integral (PI) controller. This specific controller was selected because of its simplicity in implementation and it only requires two tuning parameters (controller coefficients), i.e. Ki (integrator coefficient) and Kp (proportional coefficient). These quantities are directly and indirectly affect cost, hence levelized cost of energy (LCOE), and the design of the PTO. Additionally, the two tuning parameters are directly related to the real power (i.e. damping) and reactive power and stored energy (i.e. spring). Using the PI controller enabled us to experimentally measure the effects of changing the values of these tuning parameters on the absorbed power, PTO force, and oscillation amplitude.

The experiments have been carried out by sweeping through a number of combinations of the tuning parameter pair (Ki, Kp), to enable us to develop contour maps that shows the relationship between the controller coefficients, in the x and y axes, and performance metrics, such as the average absorbed power, the root mean square (rms) value of the PTO force and the rms value of the oscillation amplitude (or the total stroke of the PTO), in the z axis. These maps, presented in section IV, were built for a number of sea states and can be used to determine the optimal controller gains for each sea states. It is generally assumed that the optimal controller coefficients are the ones that maximize the absorbed power; however, this result is not always transferable to a larger scale device. In particular, for small scale models it is generally not feasible to build a model of the PTO with enough fidelity that is representative of its full scale version.

In contrast, hydrodynamic models can be scaled with a good degree of accuracy. Therefore, at a small scale, the hydrodynamic part of the device has to be tested separately from the PTO (this is the approach adopted for this study).

The effects of having a realistic PTO implemented in the device can be emulated by detuning the controller coefficients from the values that provide maximum hydrodynamic power absorption. In particular, a detuning of the damping coefficient corresponds to a reduced (non-ideal) efficiency of the PTO due to losses, while a reduction of the optimal reactive power term (Ki) corresponds to a PTO that is not capable of storing and providing the necessary power for maximizing hydrodynamic absorption. Thus, collecting an appropriate amount of data to build maps that cover a wide range of values for the coefficients provides useful information for the design of the PTO. It is easy to see how these maps are also connected (not necessarily in a straightforward manner) to LCOE; in fact, a larger amount of stored energy and reactive power, and a higher efficiency of the components are both associated to higher cost and absorbed power.

The block diagrams in Fig. 5 describes the location of the main sensors used for the derivation of the contour maps shown in Section IV. These sensors are a motor encoder, used to measure relative displacement and velocity of the buoys, and a load cell, used to measure the reaction force of the mooring line against the PTO. By using these sensors, characterizing the part of energy flow relative to the hydrodynamic side of the device became feasible.

IV. RESULTS AND DISCUSSION

A. Static tests: check consistency of data

This section shows the results of "integrity check" experiments that were conducted at the beginning of each test day before starting the main tests. These experiments consist of a sequence of three slowly varying ramps of different amplitude in commanded torque to the PTO motor, to verify that the WEC behaves consistently for the duration of the tests. The plots in Fig. 6 and Fig. 7 show the response of the relative displacement and the reaction force of the mooring line for the last ramp of the sequence, during the days when the data used in this report has been collected. As an additional integrity check it is possible to use these measurements to estimate the hydrostatic coefficient of the device; assuming the diameter of the buoy is equal to 0.7 m, then the hydrostatic coefficient can be calculated analytically as 3775 N/m. Fig. 8 shows the plot of displacement vs force, and the hydrostatic coefficient can be estimated by fitting a line to the data; the slope of the line is the estimate of the hydrostatic coefficient. The estimated hydrostatic coefficient for the data collected on is 3630 N/m.
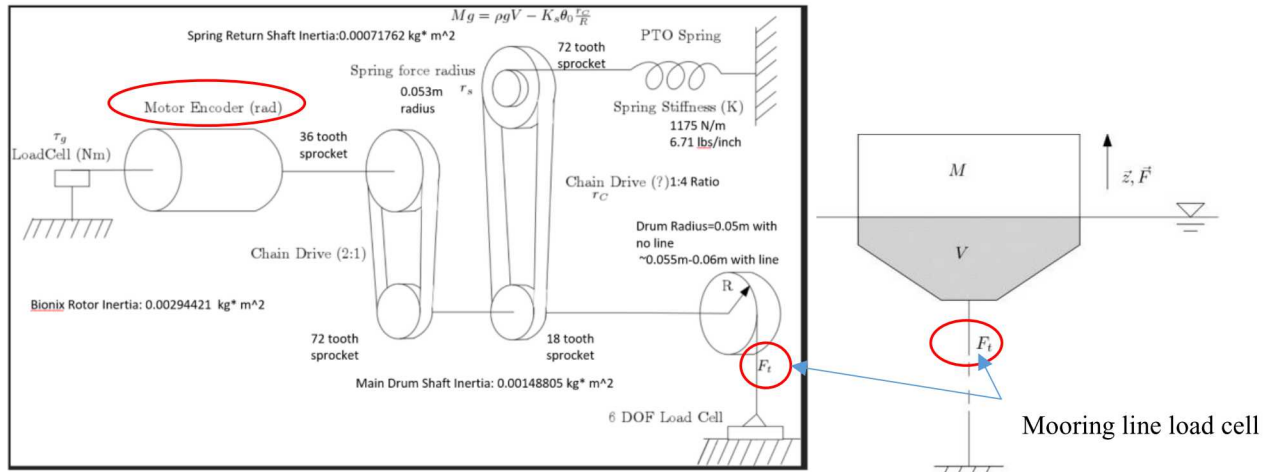
Fig. 5. Block diagram of the PTO. Highlighted in red are the locations of the motor encoder used to measure the displacement and velocity of the mooring line, and the load cell used to measure the tension of the PTO mooring line (F_t).
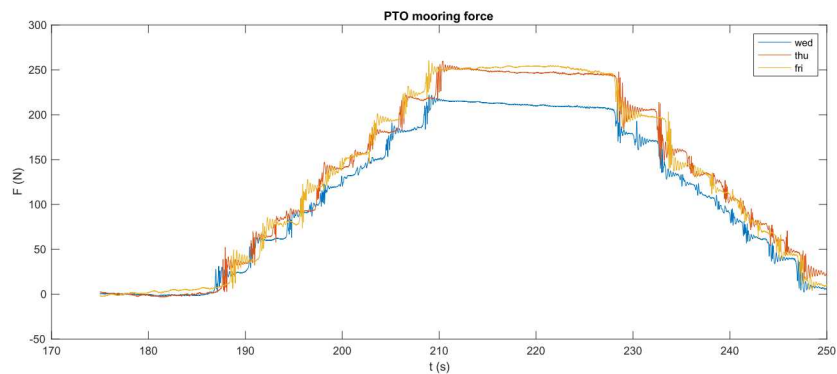

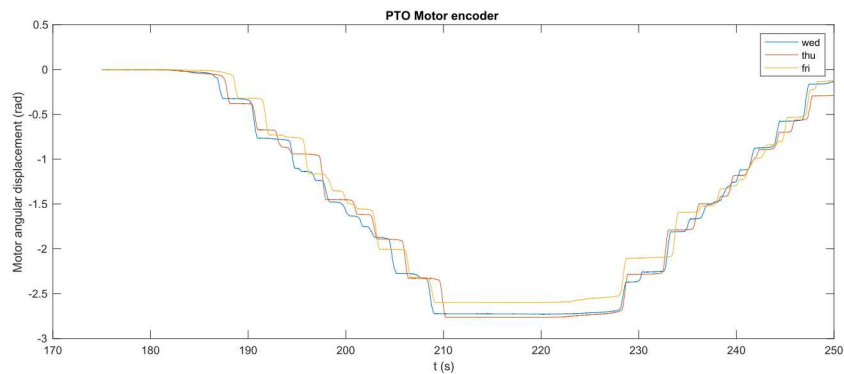
Fig. 6. PTO mooring line force during the ramp test

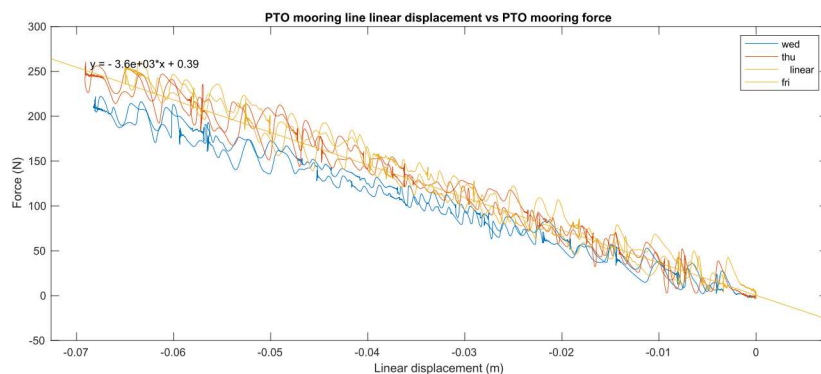Fig. 7. Angular displacement of the PTO motor during the ramp test

Fig. 8. Mooring line linear displacement vs mooring line force. The plot also shows a linear fit to one of the ramp test. The estimated hydrostatic coefficient is 3630N/m.

B. Dynamic tests: Closed loop control and parameters sweep

This section provides a description of the parameters sweep experiments, the data processing and the results. The data used for these dynamic tests is a subset of the total dataset collected during the wave tank testing campaign. In particular, the subset of experiments used for this paper is listed in Table 1; the table includes the identifier of the experiment (Exp ID) and the parameters of the Bretschneider spectra used for each test. The parameters of the spectra are also plotted in Fig. 9. It is important to note that all the results provided in this section can be scaled arbitrary by means of Froude scaling. For example, assuming that λ is the scaling factor, the data in Fig. 9 can be scaled by scaling the x axis with $\sqrt{\lambda}$ and the y axis with λ.

TABLE 1
SUMMARY OF TEST CASES, CORRESPONDING SEA STATES AND EXPERIMENTS IDENTIFIER (ID) AS LISTED IN THE TEST LOG

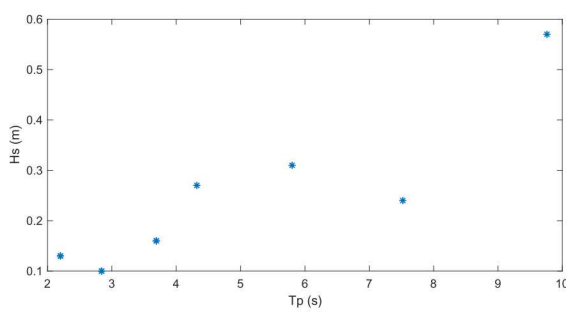| Test case	Exp ID	Hs (m)	Tp (s)
1	33	0.27	4.32
2	35	0.24	7.52
3	37	0.31	5.8
4	41	0.13	2.2
5	42	0.13	2.2
6	43	0.1	2.84
7	44	0.1	2.84
8	45	0.16	3.69
9	46	0.16	3.69
10	55	0.57	9.76

Fig. 9. Sea states.

The parameters sweep tests have been carried out by first generating a repeating sequence for the water surface elevation; that is, during each experiment, the wave maker is repeating the same sequence a number of times. Each sequence is characterized by the spectrum and the duration T_r; the duration is $T_r = 200s$ for test cases 1-9, and $T_r = 300s$ for test case 10 (test case 10 has a much lower peak frequency). The spectrum is Bretschneider and the parameters (Hs and Tp) for each experiment are listed in Table 1. During each experiment the control system is preprogrammed to sweep through a set of coefficients pair

(Ki and Kp); the coefficients are updated periodically with an update time equal to the length of the wave sequence T_r. Note that the sea state for test case 4 and 5 are the same, but the mooring line pre-load between both tests are different. Similarly, this condition also applies to test cases 6 and 7, and 8 and 9. This was done for investigating the sensitivity of performance to the WEC equilibrium position and stroke.

The control system sends a command to the motor controller and the motor applies the desired torque to the shaft. The torque applied to the motor is, however, different from the torque at the drum (or to the force applied to the mooring line multiplied by the radius of the drum) because of the friction in the drivetrain (bearings, gearing etc.), inertia of the motor and the return spring. This is typical for small scale prototypes, but it is not a source of concern with regards to the quality of the data collected during the experiment and for the validity of the results, for two reasons: 1) We can measure directly the quantities of interest (i.e. Mooring line force Ft and PTO angular velocity); 2) the PTO system (sensors, actuation, drivetrain, I/O and real-time system) has been designed to achieve good performance of torque tracking at the motor shaft, thus the motor can apply very accurately the commanded torque. In this situation, because of the non-negligible dynamics of the drivetrain, there will be a mismatch between the control law applied at the shaft and the effective Ki and Kp applied at the mooring line, which will be used for the evaluation of the hydrodynamic performance of the device. However, the mismatch is only due to the dynamics of the drivetrain, since the motor does not introduce significant artifacts. In this situation, the effective Kp (damping) and Ki (spring) applied to the buoy can be accurately estimated from the data.

The effective values of the controller's coefficients (Ki_m and Kp_m) applied to the buoy by the mooring line can be estimated starting from the following model:

$$\tau_t = \tau_{0m} - Ki_m\,\theta - Kp_m\,\omega,$$

Where τ_t is the torque at the drum and it can be measured by multiplying the load cell measurement (F_t) by the radius of the drum; τ_{0m} is the pre-load torque; θ is the angular displacement of the drum that is measured by the motor encoder multiplied by the gear ratio of the chain drive (2:1); ω is the angular velocity of the drum. The model is linear in the coefficients that need to be estimated (τ_{0m}, Ki_m, Kp_m); therefore, the simple least squares algorithm can be used for the estimation.

Fig. 10 shows the estimated coefficients during each sequence of the experiment for each test case; each experiment is composed of 16 sequences, for a total durations of 16*T_r =3200s. Plot also shows the commanded coefficients applied by the motor: it is possible to see the discrepancy between Kp_m and Kp_c due to the friction, between Ki_m and Ki_c due to the air spring and inertia, and

between τ_{0m} and τ_{0c} also due to the pre-load provided by the air-spring.

Fig. 11 shows the average absorbed power as function of the estimated Ki_m and Kp_m coefficients (red asterisks). The surface has been built by fitting a 3rd degree 2-dimensional polynomial to the data, and it helps to visualize the pattern of power vs controller's coefficients. The polynomial fitting was also used to plot the contour lines in Fig. 12; the same figure also shows the contour lines of the map between rms value of the angular displacement and Ki_m, Kp_m, and the map between the rms value of the mooring torque and Ki_m, Kp_m. These maps will be used for the design of the optimal PTO and control system for this device (control co-design). In fact, a given configuration of the PTO and control system will be mapped into an equivalent Ki_m and Kp_m, thus allowing the coupling of the hydrodynamic model with the PTO and control system for evaluating power, stroke, force, and eventually cost.

REFERENCES

[1] Department of Energy (2016). Wave Energy Prize Official Webpage [Online]. Available: (https://www.energy.gov/eere/water/wave-energy-prize-home).

[2] Yu, Yi-Hsiang, Ruehl, Kelley, Van Rij, Jennifer, Tom, Nathan (2015). Wave Energy Converter SIMulator (WEC-Sim) online web page [Online]. Available: https://wec-sim.github.io/WEC-Sim/theory.html
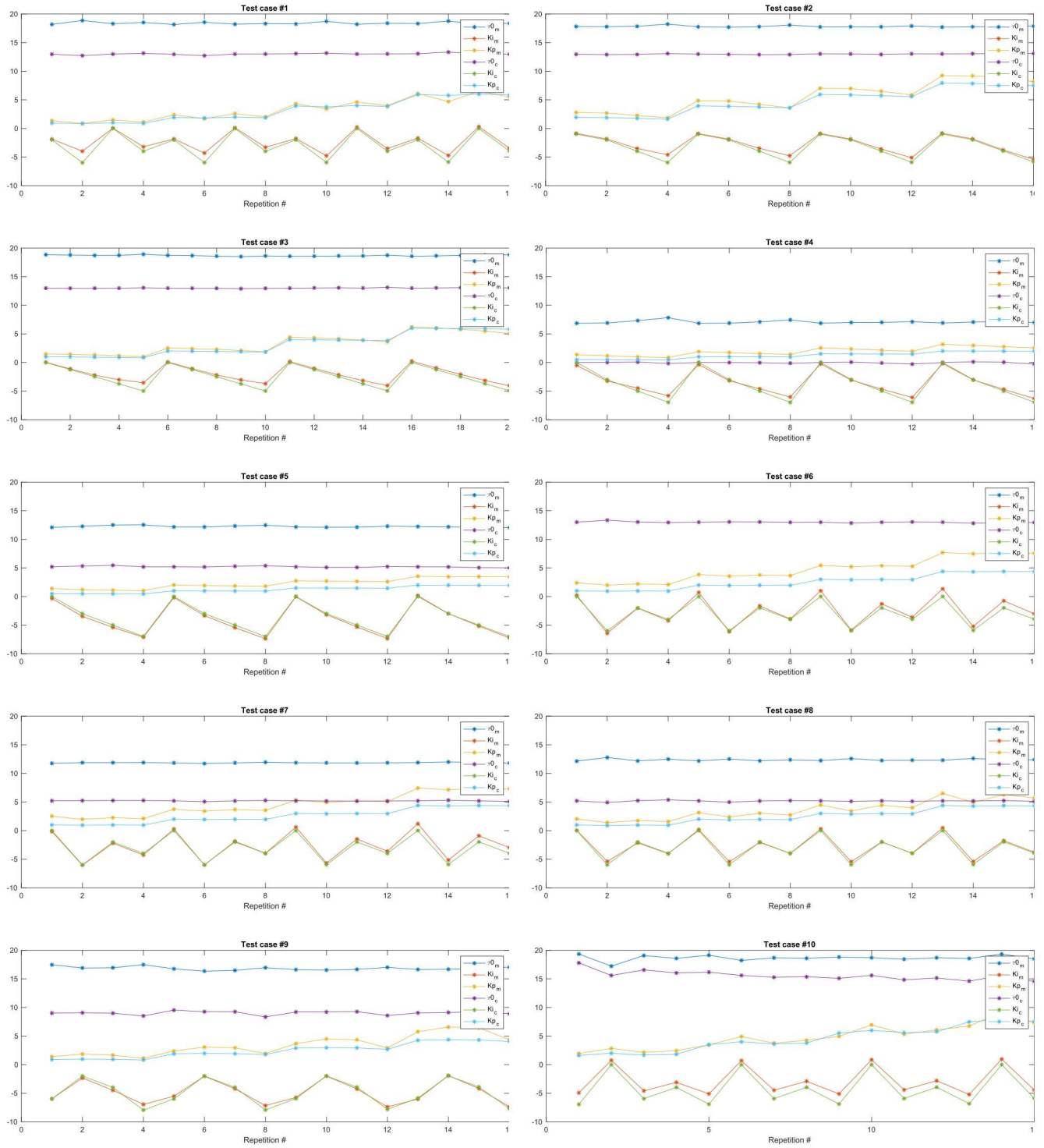
Fig. 10. Estimated control coefficients for each repetition. The duration of each repetition is 200s.
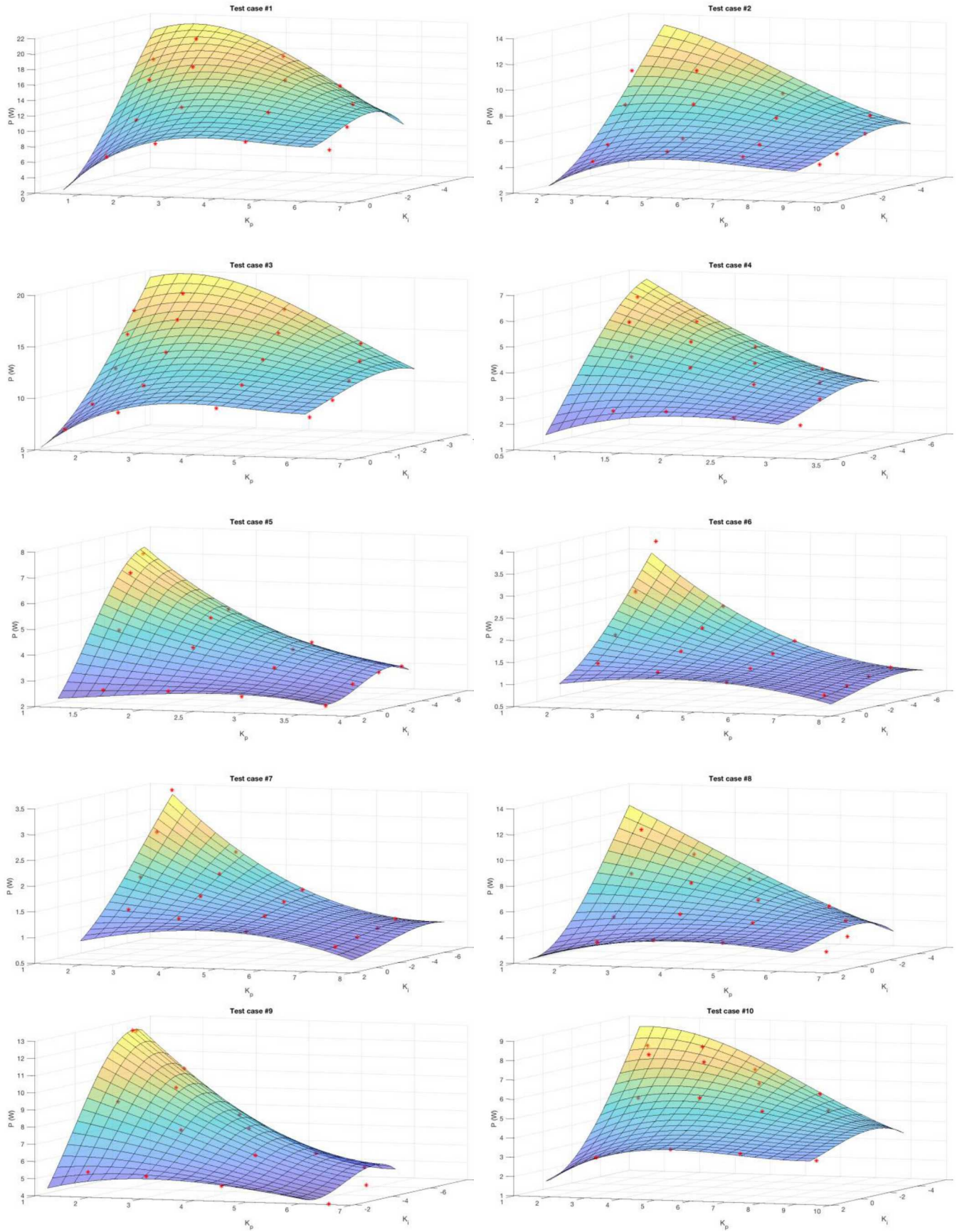
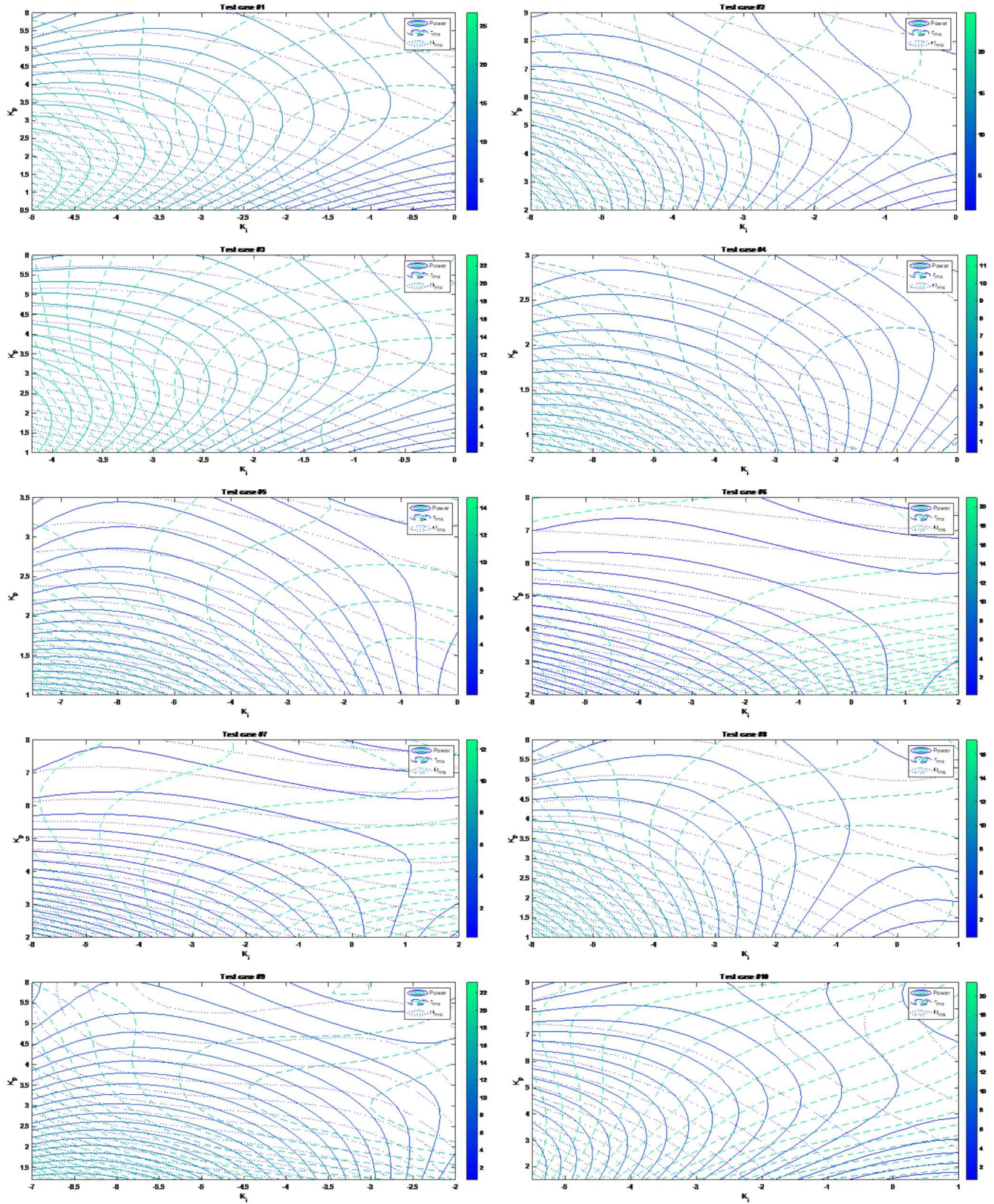Fig. 11. Absorbed power as function of the control coefficients.

Fig. 12. Contour plots of the absorbed power, rms value of the PTO torque, rms value of the angular displacement.